Interfacial tension of ethanol, water, and their mixtures in high pressure carbon dioxide: measurements and modeling

Aymeric Fabien, Guillaume Lefebvre, Brice Calvignac, Pierre Legout, Elisabeth Badens, Christelle Crampon

Interfacial tension of ethanol, water, and their mixtures in high pressure carbon dioxide: measurements and modeling

Aymeric Fabien[a], Guillaume Lefebvre[b], Brice Calvignac[b], Pierre Legout[b], Elisabeth Badens[a*], Christelle Crampon[a]

[a] **Aix Marseille Univ**, CNRS, Centrale Marseille, **M2P2**, Marseille, France

[b] **Univ Angers**, Inserm, CNRS, **MINT**, SFR ICAT, F-49000 Angers, France

* Corresponding authors

Abstract

Hypothesis: It is particularly noteworthy to study interfacial tension behavior under pressurized carbon dioxide for supercritical processes such as crystallization or fractionation. For the latter, a liquid phase and a supercritical phase are in contact, and interfacial properties influence mass transfer phenomena and hydrodynamics. Ethanol-water mixture is a good theoretical study case also involved in a wide range of applications.

Experimental: Interfacial tensions of ethanol, water and three mixtures, with an ethanol mass fraction from 0.25 to 0.75, under pressurized CO_2 were measured for pressures ranging from 0.1 MPa to 15.1 MPa at 313.15 K and 333.15 K. A specific experimental set-up was used for CO_2 phase saturation.

Findings: This work brings interfacial tension data of five different solutions including water and ethanol in contact with CO_2. Effects of pressure, temperature, carbon dioxide density and ethanol mass fraction are discussed regarding the literature. Significant discrepancies are found with previous literature data for ethanol-water mixtures. The "two-step" decrease observed when pressure or density increase is also discussed regarding both the concept of Widom line, and the polar and dispersive contributions of the surface tension of a component. For the first time, fair accurate interfacial tension modeling involving these contributions is addressed.

Keywords:

Interfacial tension measurement, modeling, high pressure, ethanol-water mixture, supercritical carbon dioxide

1. Introduction

Interfacial properties such as gas-liquid, or liquid-liquid interfacial tensions are useful in a wide range of processes like separation. From a chemical engineering point of view, these properties are for instance involved in drop or bubble size distribution and therefore linked to the contact area, which is directly connected to transfer phenomena that take place at the interface. The influence of interfacial tension on hydrodynamics, like the flooding phenomenon, is also of high importance. Indeed, if the influence of interfacial tension on hydrodynamics is debatable in the case of gas-liquid contactors [1], even simply neglected, this parameter plays a role on the flooding capacity in the case of liquid-liquid systems [2,3]. Consequently, interfacial tension is of great importance in such processes for design and modeling.

High-pressure carbon dioxide (CO_2) is commonly used for supercritical fluid (SCF) technology and an increasing interest is being seen for it to be one alternative to the conventional processes which use liquid organic solvents. SCF processes take advantage of the specific properties of supercritical fluids: liquid-like densities; gas-like viscosities; diffusion coefficients higher than in liquids, which give them valuable solvent properties. Numerous data about physicochemical properties are now available, especially for systems involving supercritical carbon dioxide which is the most encountered SCF. One particular feature of systems involving a supercritical phase is the significant decrease of interfacial tension, even to its vanishing, according to the conditions of pressure and temperature. Overviews of interfacial tension measurements under supercritical CO_2 conditions can be found [4,5] for various systems such as water, alcohols or oils and derivatives. Its knowledge is of great importance to accurately describe numerous processes, particularly separation processes such as supercritical fractionation or crystallization. For fractionation, since it is generally conducted in counter-current packed columns, a deep knowledge of the interfacial phenomena between the two phases involved is of interest to study either the mass transfer kinetics [6] or hydrodynamics and flooding [7]. Regarding supercritical crystallization processes, especially for supercritical antisolvent ones (SAS), an effective control of the end-product characteristics necessarily includes the description of hydrodynamics [8–10] which requires the knowledge of interfacial properties. Recently, modeling has been used to estimate interfacial tensions in the framework of organic nanoparticle formation in a microfluidic system (microSAS) [11].

In order to study the behavior of interfacial tension in supercritical CO_2 (SC-CO_2) media, an ethanol-water system was chosen. Indeed, it is both well described in the literature and also of industrial interest for high concentrated ethanol production or the removal of ethanol from beverages, by the use of SC-CO_2 fractionation process. Since ethanol-water composition varies on a large scale along the fractionation column, it is of great interest to characterize the interfacial tension properties for several compositions that may impact transfer phenomena and hydrodynamics. However, from the best of our

knowledge, interfacial tension measurements in SC-CO_2 environment were carried out with pure water and/or brine [9,12–27], mainly for geological storage applications, or with pure ethanol [12,28–31]. In contrast, little data are available for interfacial tensions of ethanol-water mixtures in pressurized CO_2 [12,15], which present significant differences with data under atmospheric conditions [32] at the same pressure and temperature.

Consequently, an experimental campaign was performed to measure the interfacial tensions in dense CO_2 for water, ethanol, and their mixtures for a total of three different ethanol mass fractions, noted ω, of 0.25, 0.50 and 0.75. Experimental conditions for interfacial tension measurements were chosen to be in accordance with operational conditions applied in the fractionation process for ethanol-water separation using SC-CO_2 [33–35], with pressure up to 15.1 MPa and temperature of 313.15 K and 333.15 K. These measurements were expected to provide reliable data for ethanol-water systems in contact with SC-CO_2, and to enhance the comprehension of the interfacial tension behavior depending on pressure, temperature, carbon dioxide density and mixture composition.

This work first describes the experimental set-up used for interfacial tension measurements with the followed procedure. The results are then presented according to pressure, temperature, carbon dioxide density as well as the composition of ethanol in the mixture. Results are compared to literature data available on this topic. New assumptions considering the potential influence on interfacial tension behavior in pressurized CO_2 of both the Widom line as well as the polar and dispersive contributions of the surface tension are also discussed. Finally, useful correlations enabling us to describe interfacial tension behavior through these studied parameters were also proposed.

2. Materials and methods

2.1 Definitions

Interfacial tension or interfacial energy between two immiscible phases 1 and 2 in contact, noted γ_{12}, is the free energy variation when the contact surface is enlarged by unit area [36]. In this work, interfacial tensions denoted γ_{LF} generally mean liquid-fluid interface, including liquid-vapor and liquid-supercritical fluid interfaces.

If the phase 2 is air or vacuum, this property is called surface tension or surface energy and is commonly denoted γ_L for a liquid and γ_S for a solid. The surface tension of a component phase *i*, denoted γ_i, can be seen as the addition of different contributions, the dispersive one, denoted γ_i^d, and the polar one, denoted γ_i^p as shown in Eq. (1).

$$\boldsymbol{\gamma_i = \gamma_i^d + \gamma_i^p} \qquad (1)$$

Surface tension data of ethanol and water with their dispersive and polar contributions at 293.15 K and 311.15 K [37] are presented in Table 1.

2.2 Materials

Measurements of interfacial tension were realized with ultrapure water (Merck) with a resistivity of 18.2 MΩ.cm and absolute ethanol (VWR Chemicals) with purity higher than 99.8%. The same reagents were used to prepare the mixtures by weighing with a high precision balance. Three ethanol mass fraction mixtures of 0.25, 0.5 and 0.75 were studied. The carbon dioxide used during the experiments was high grade, greater than 99.9% purity (Linde).

2.3 Experimental set-up description

Numerous methods based on force balance can be used to measure interfacial tensions [38,39]. The pendant drop method is widely used to estimate interfacial tension under pressure and is the one that was chosen for this work coupled with a picture analysis software (Teclis ®). This software allows the determination of the interfacial tension by analyzing the axial symmetric shape (Laplacian profile) of the pendant drop [40] and the well-known Young-Laplace equation [41].

The experimental setup allowing interfacial tension measurements with pendant drop method under pressurized carbon dioxide atmosphere, for pressure and temperature up to 35 MPa and 473.15 K, respectively, is presented in Fig. 1, and was previously validated for water-CO_2 interfacial measurements in presence, or not, of polymeric surfactants [42].

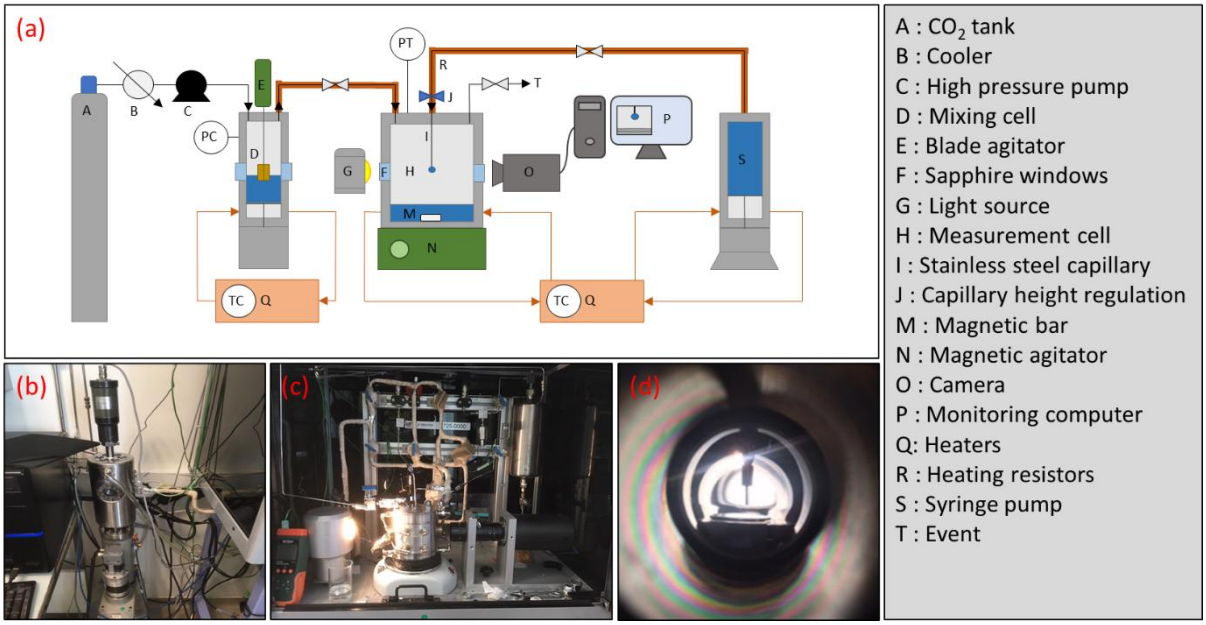

Fig. 1 Experimental setup for interfacial tension measurements at elevated pressures and temperatures. (a) Schematic diagram, (b) photograph of the mixing cell, (c) photograph of the measurement cell and optical system, (d) photograph of inside measurement cell.

The pressurization system is composed of a CO_2 tank (A), a cooler (B) and a high-pressure pump (C) (Separex). The setup is composed of a mixing and motorized variable volume pump cell (D), a measurement cell (H) (Top Industrie), and a syringe pump (S) Teledyne Isco 260D (Serlabo Technologies), all equipped with double envelopes. The optical system is composed of a CCD camera (O) connected to a computer (P), and a light source (G).

The measurement cell disposes of a stainless-steel capillary or needle (I) with height regulation (J), and two sapphire windows (F) where the light source and the CCD camera are face to face.

During experiments, the syringe pump (S) was filled with the studied mixture as well as the bottom of both cells (D and H) to ensure quicker saturation of the carbon dioxide, by using a blade agitator (E) in the mixing cell and a magnetic agitator in the measurement cell (respectively M and N), and thus to reduce the time to reach saturation of the CO_2.

The pressure was kept constant thanks to a piston in the mixing cell and the temperature was kept constant thanks to two heating baths (Q) that fed the double envelopes and heating resistors (R) along the tubing between each part of the apparatus.

2.4 Measurement procedure

Interfacial tensions were measured for five solutions: pure water and ethanol and three different ethanol-water mixtures with an ethanol mass fraction of 0.25, 0.50 and 0.75, in presence of carbon dioxide under various pressures from 0.1 to 15.1 MPa at 313,15 and 333.15 K. Each measurement was carried out at least in triplicate and the average value was retained; the repeatability uncertainty is therefore calculated for 99% of confidence level.

The calculation of interfacial tension by pendant drop method requires us to know the densities of both the liquid and continuous phases. The experimental set-up is not designed to measure the densities of the saturated phases; therefore, densities were calculated from pure compound data. This way is widely used in the literature and allows well-defined data. Pure compound densities at given pressure and temperature were taken from the National Institute of Standards and Technology (NIST) for carbon dioxide and water, from Watson et al. [43] for ethanol, and interpolated for ethanol-water mixture from Pečar et al. [44]. These thermodynamical data are given in supplementary files (A-Table 2).

At first, the bottom of both the mixing cell and the measurement cell were filled with the studied mixture. The set-up was then closed and flushed with CO_2 for a few minutes to remove the air, and finally the pressure and temperature were set. Passing through the mixing cell, the CO_2 was "pre-saturated" with the studied mixture. After 30 to 60 minutes to reach saturation of CO_2 phase, a drop was generated at the end of the capillary thanks to the syringe pump with low flowrate to control the drop volume. As long as the drop was stable, it was maintained at the end of the capillary for about ten

minutes, to ensure CO_2 transfer into the liquid phase [25]. This procedure allows us to measure static interfacial tension values (independent of time and drop volume), as described in the work of Hebach et al. [18]. Because reaching the true thermodynamical equilibrium remains currently discussed in the interface science community (Hinton et al. [45]), we prefer to use "static" term. This type of "static" values offer the advantage of well reproducible measurements [18].

The Bond number (*Bo*) or form factor characterizes the shape of the pendant drop in comparing gravity to capillary forces and is defined as follows in Eq. (2).

$$Bo = \frac{\Delta\rho.g}{\gamma_{LF}.b^2} \qquad (2)$$

Where $\Delta\rho$ is the density difference between the two fluids and b is the inverse of curvature radius at the apex of the drop. If the $Bo < 0.1$, the capillary forces dominate and the drop is then more spherical, and if the $Bo > 1$ the gravity forces dominate, and the drop has a more elongated shape. Consequently, *Bo* must be between 0.1 and 1 [40,46]. The *Bo* was calculated with values in the right range from 0.1 to 0.7.

3. Results and discussions

3.1 Pressure effect

The interfacial tension measured at the liquid-fluid interface of ethanol, water, and their mixtures in presence of pressurized carbon dioxide are presented as a function of pressure in Fig. 2, Fig. 3, and Fig. 4, respectively, and compared with the available literature data.

For the CO_2/ethanol system at 313.15 K and 333.15 K (Fig. 2(a) and Fig. 2(b), respectively), results agree with the literature. It appears that the CO_2/ethanol interfacial tension decreases almost linearly for both temperatures up to around 8 MPa at 313.15 K and 10 MPa at 333.15 K where the value becomes practically null.

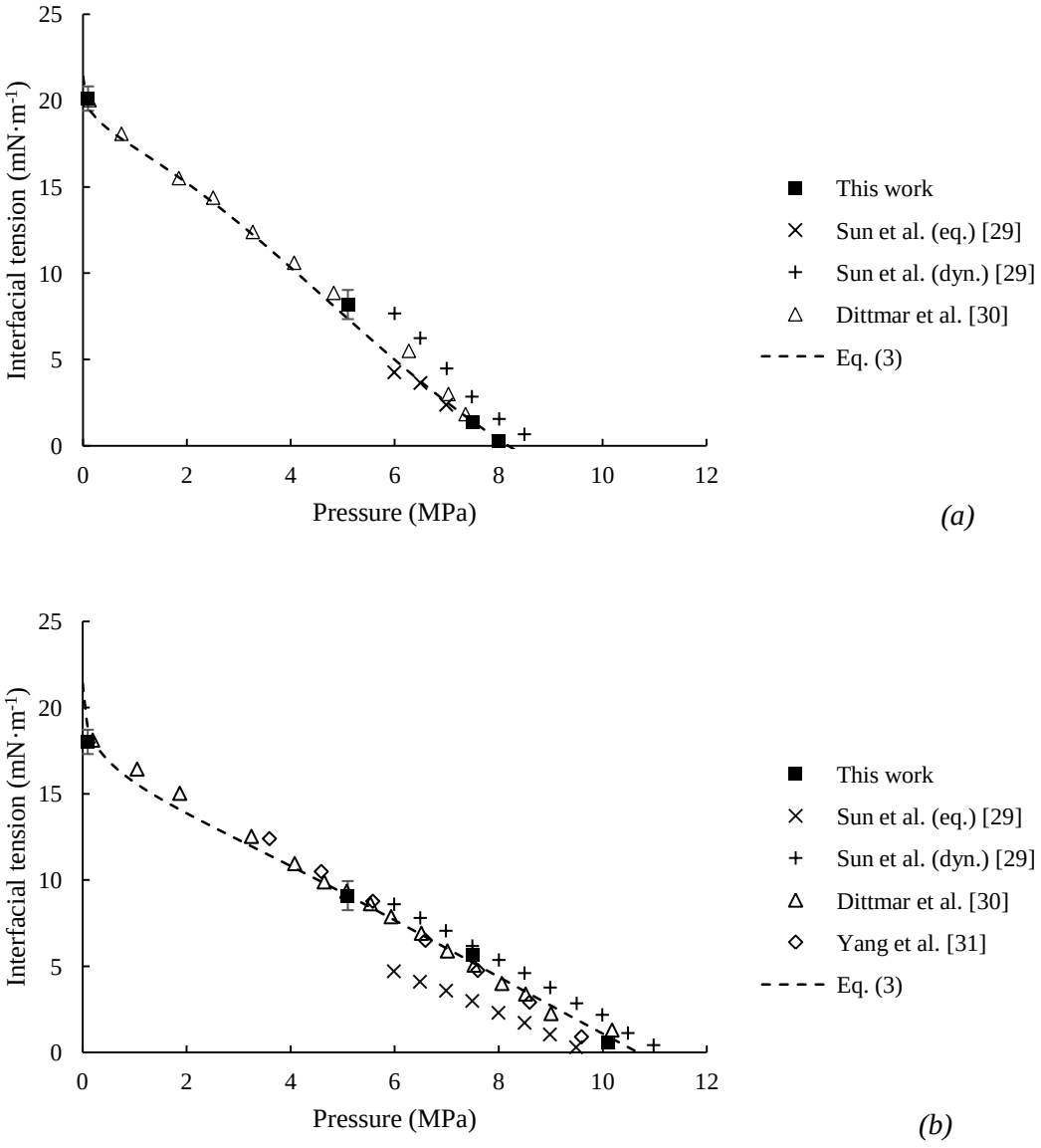

Fig. 2 Interfacial tensions for CO_2/ethanol systems at (a) 313.15 K; (b) 333.15 K. Correlation is given by Eq. (3).

Beyond these pressures with respect of temperature, drop formation was not possible due to the very low values of interfacial tensions and measurements were no longer feasible. This phenomenon is explained by the formation of a jet instead of a drop in the work of Dittmar et al. [30], and by reaching the minimal pressure for which the two compounds are miscible in the work of Yang et al. [31].

Concerning the CO_2/water system at 313.15 K and 333.15 K (Fig. 3(a) and Fig. 3(b), respectively), the results agree with the most of literature data, and discussion on discrepancies, including recent findings [45], is given in supplementary files B. From a phenomenological point of view CO_2/water interfacial tension decreases according to two steps, with a significant slope variation. Indeed, from 0.1 to around 8 MPa at 313.15 K, and around 10 MPa at 333.15 K, the interfacial tension decreases strongly with pressure, while at higher pressure, the interfacial tension decreases slowly following asymptotic-like behavior.

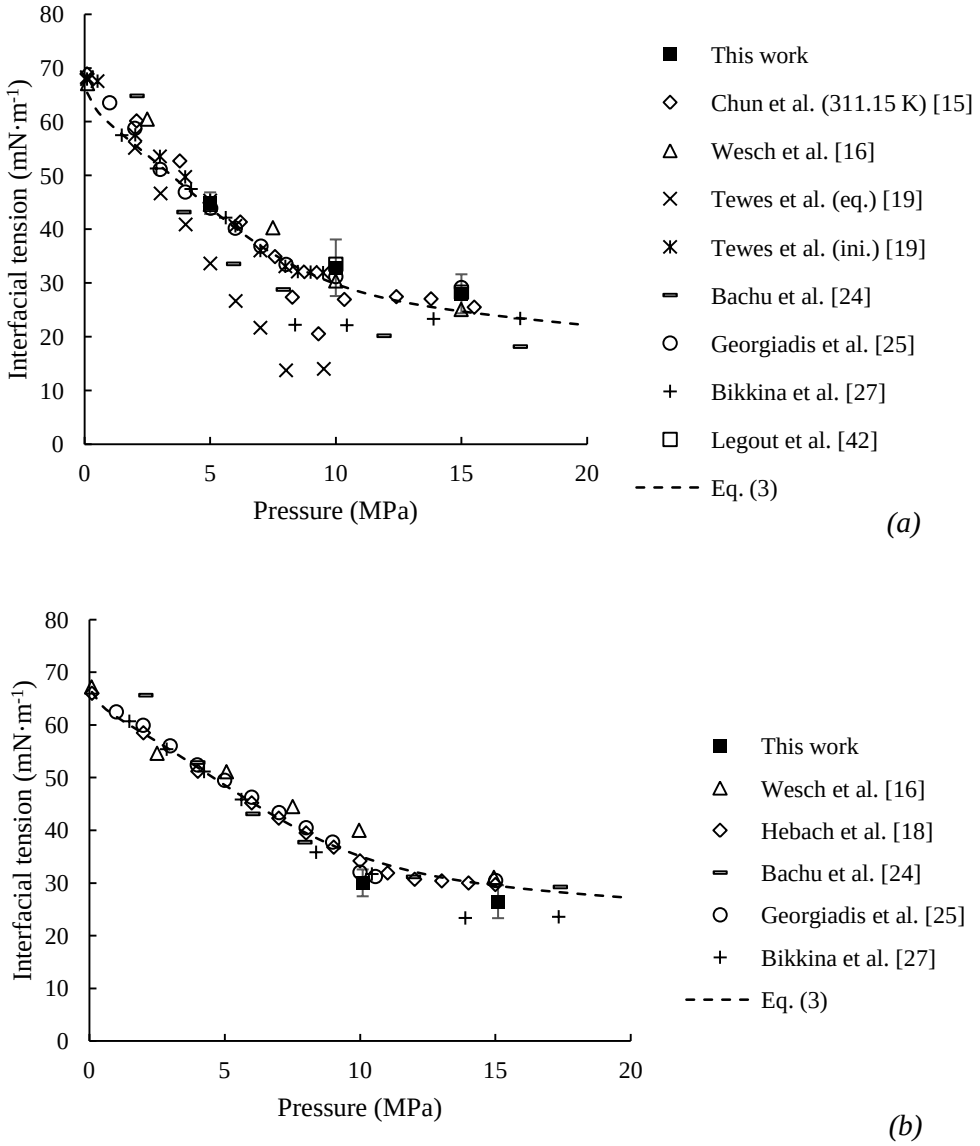

Fig. 3 Interfacial tensions for CO_2/water systems at (a) 313.15 K; (b) 333.15 K. Correlation is given by Eq. (3).

Interfacial tension measurements for CO_2/ethanol-water mixtures at 313.15 K and 333.15 K are presented in Fig. 4(a) and in Fig. 4(b), respectively. The decrease behavior is like that described for the CO_2/water system, with decreasing values as the ethanol content increases.

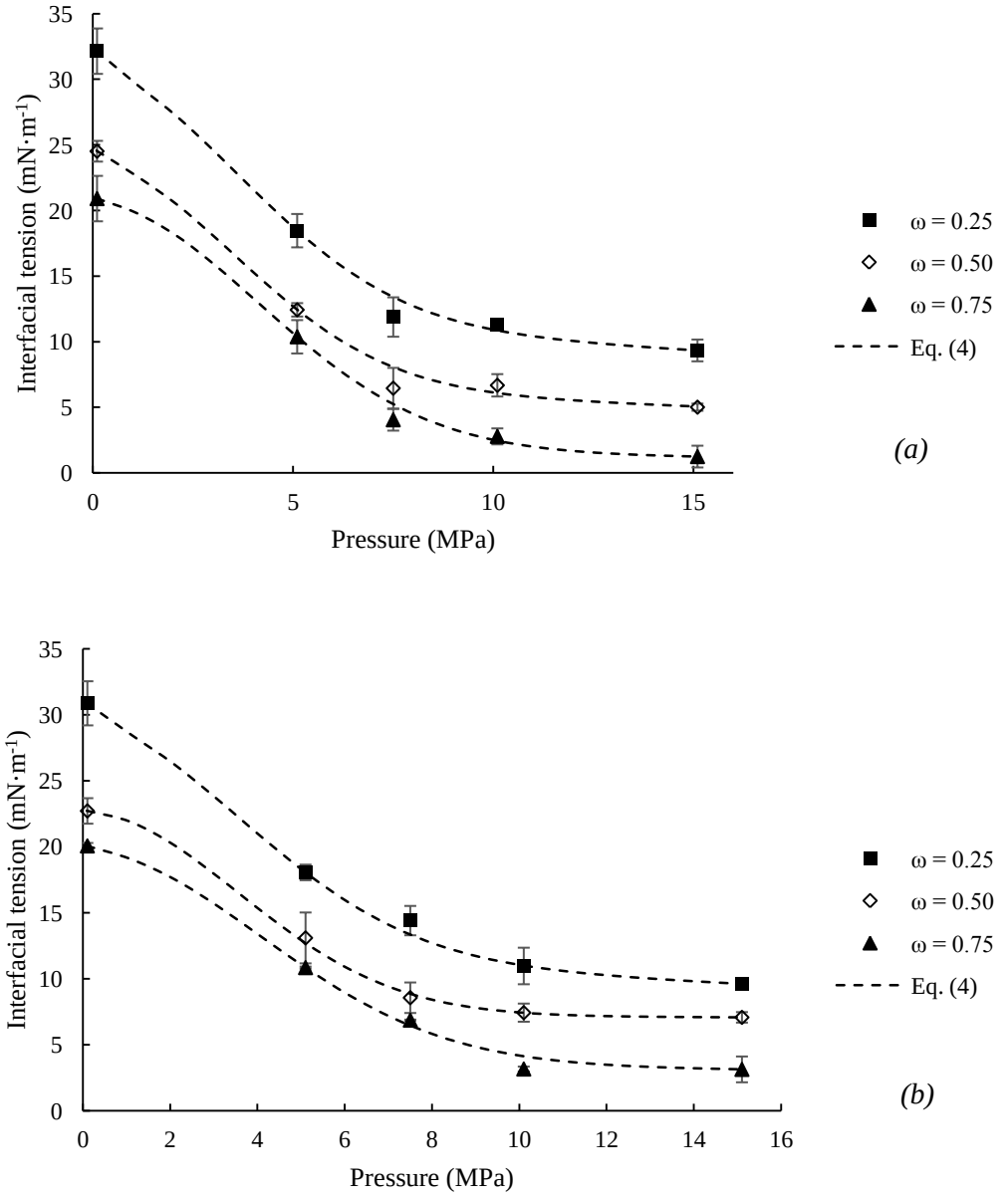

Fig. 4 Interfacial tensions for CO_2/ethanol-water mixtures at (a) 313.15 K; (b) 333.15 K. Correlation is given by Eq. (4).

This two-step behavior has already been discussed in the literature and a relation with the CO_2 solubility in water was proposed in the work of Sutjiadi-Sia et al. [12]. This behavior has also been directly linked to the CO_2 critical point in the work of Bachu et al. [24] but was not observed for all conditions in this work. Indeed, at 313.15 K the transition appears near the critical pressure of CO_2, however at higher temperature the transition appears at higher pressure (on the average of 10 MPa). Georgiadis et al. [25] linked this phenomena to a local maximum of CO_2 isothermal compressibility factor with a corresponding pressure of 8.75 and 10.4 MPa at 312.9 K and 333.5 K, respectively, in agreement with the observations made in this work.

In order to link these different observations and assumptions, it is worth mentioning here that above the critical point, in the supercritical domain, there is a boundary line, called the Widom line [47,48],

that separates a zone where the SCF has liquid-like properties from a zone where it has gas-like properties. This line is the locus of discontinuous changes in fluid properties. This line vanishes for higher pressure and temperature. For carbon dioxide, the end-point of the Widom line corresponds to a pressure lower than 10 MPa [48]. Thus, the zone of pressure lying from the critical pressure and the end-point pressure of the Widom line delimits a range where the properties such as the interfacial tension can exhibit a specific behavior. Crossing the Widom line could lead thus to this two-step behavior.

3.2 Temperature effect

Due to the narrow temperature range studied and uncertainties, the effect of temperature cannot be well discussed using only the data presented in this work. Nonetheless, temperature effect can be seen in three steps as presented in the Fig. 5 for the CO_2/water system with data from Georgiadis et al. [25].

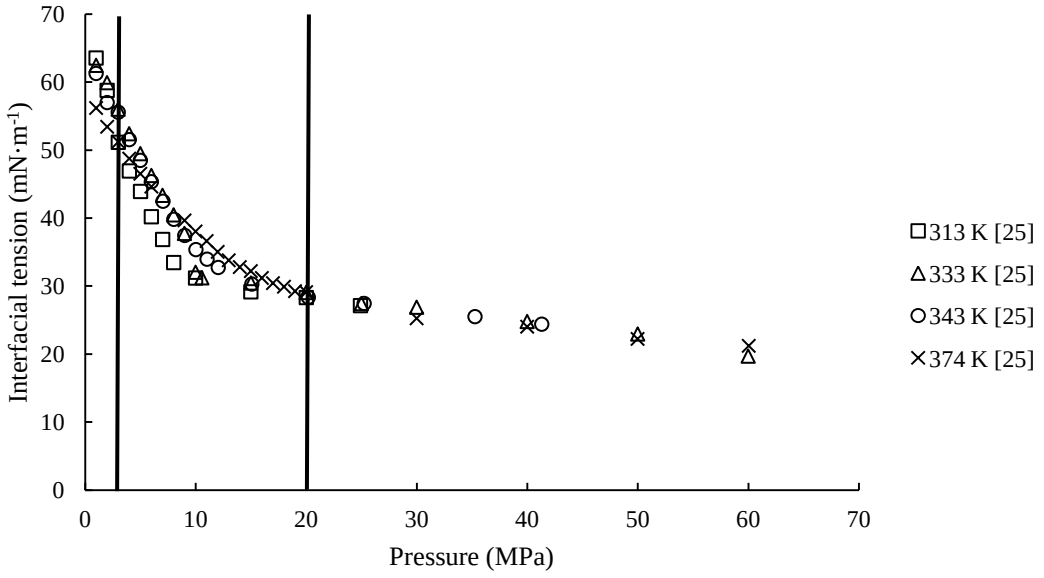

Fig. 5 Isotherms of CO_2/water interfacial tensions from Georgiadis et al [25].

First, it is well known that under atmospheric conditions the interfacial tension decreases linearly when the temperature increases, for instance this behavior is shown for ethanol-water mixtures in the work of Vazquez et al. [32]. During an intermediate step, from low pressure to around 20 MPa, it appears that when the pressure increases, the temperature has an opposite effect as it can be seen for CO_2/ethanol or CO_2/water, with a maximum difference around the critical pressure of CO_2. In this intermediate step, interfacial tension appears to be density dependent as shown in Fig. 6. Finally, for density higher than 600 kg·m^{-3}, experimental points are dispersed according to the temperature in Fig. 6(b) while the interfacial tension of CO_2/water appears only pressure dependent for pressures higher than 20 MPa as shown in Fig. 5.

3.3 Carbon dioxide density effect

Interfacial tension can be plotted as a function of carbon dioxide density and appears to be temperature non-dependent except at low density. This relation between carbon dioxide density and interfacial tension has already been observed and discussed in the work of Dittmar et al. [30] for various systems, including ethanol and water, and remains valid for temperature beyond the critical temperature of CO_2 and density higher than 20 $kg \cdot m^{-3}$. Datasets of CO_2/ethanol and CO_2/water interfacial tensions are respectively completed with data from Dittmar et al. [30] between 313 K to 351.5 K, and data from Georgiadis et al. [25] with a temperature range from 313 K to 373 K.

Interfacial tensions of studied systems as a function of the carbon dioxide density are shown in Fig. 6(a) for the CO_2/ethanol system, in Fig. 6(b) for the CO_2/water system, and in Fig. 6(c) for the CO_2/ethanol-water mixtures. It must be noted that the mixture of two density dependent solutions lead to a density dependent mixture in the case of water and ethanol. For all studied systems, interfacial tension decreases as the carbon dioxide density increases, with a first significant decrease to around 300 $kg \cdot m^{-3}$ followed by asymptotic-like behavior, except for the CO_2/ethanol system where the interfacial tension tends to zero at higher density. It can be noted through Fig. 6(b) for the CO_2/water system, that temperature might have an effect at high density, beyond 600 $kg \cdot m^{-3}$. Indeed, points are more dispersed but follow a tendency depending on temperature.

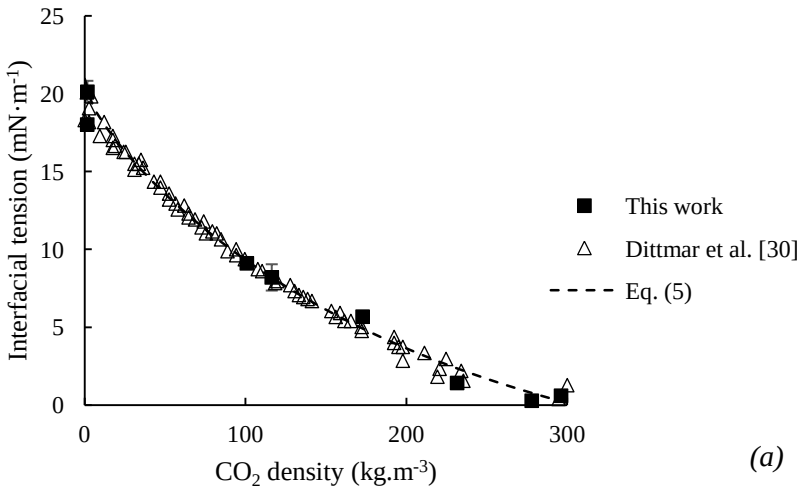

(a)

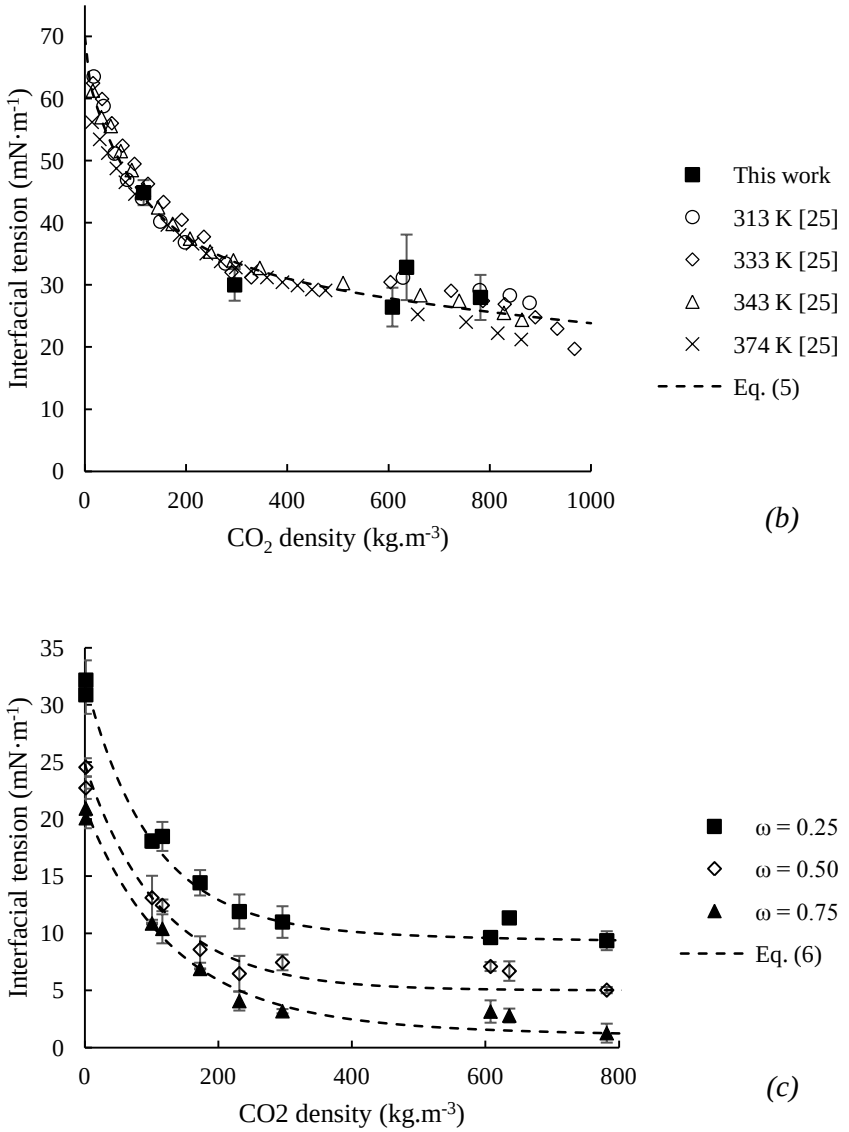

Fig. 6 Interfacial tension versus CO_2 density; (a) CO_2/ethanol system; (b) CO_2/water system - Correlation is given by Eq. (5); and (c) CO_2/ethanol-water mixtures - Correlation is given by Eq. (6).

3.4 Ethanol composition effect

Experimental interfacial tensions from this work were plotted as a function of ethanol mass fraction, for various pressures at 313.15 K and 333.15 K, in Fig. 7(a) and Fig. 7(b) respectively. Water data are completed from the literature [16,18,19,25] and interfacial tension of ethanol is supposed to tend towards zero above 7.5 MPa and 10.1 MPa at 313.15 K and 333.15 K, respectively.

Interfacial tension decreases exponentially on increasing the ethanol mass fraction. A small content of ethanol generates a significant decrease in interfacial tension, then it converges slowly towards the ethanol interfacial tension as the ethanol content increases. This behavior is observed for all pressures and both temperatures (Fig. 7(a) and (Fig. 7(b)).

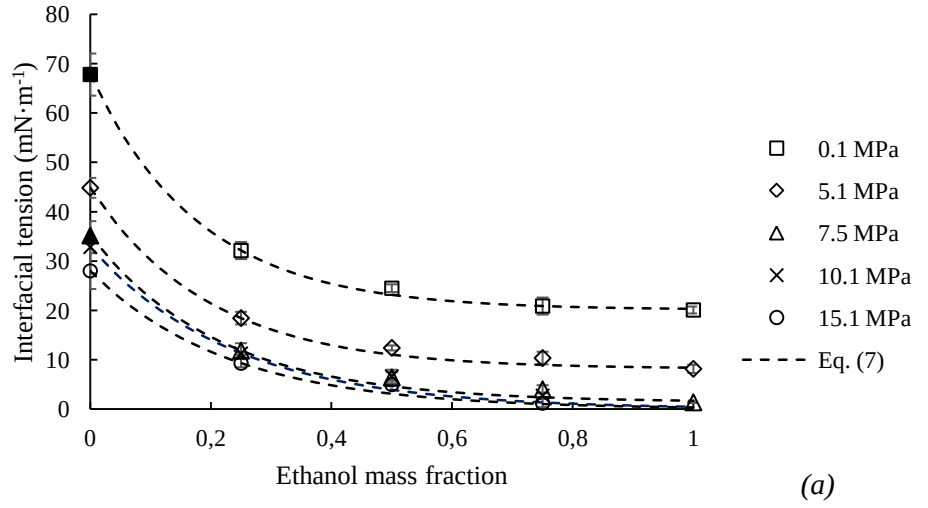

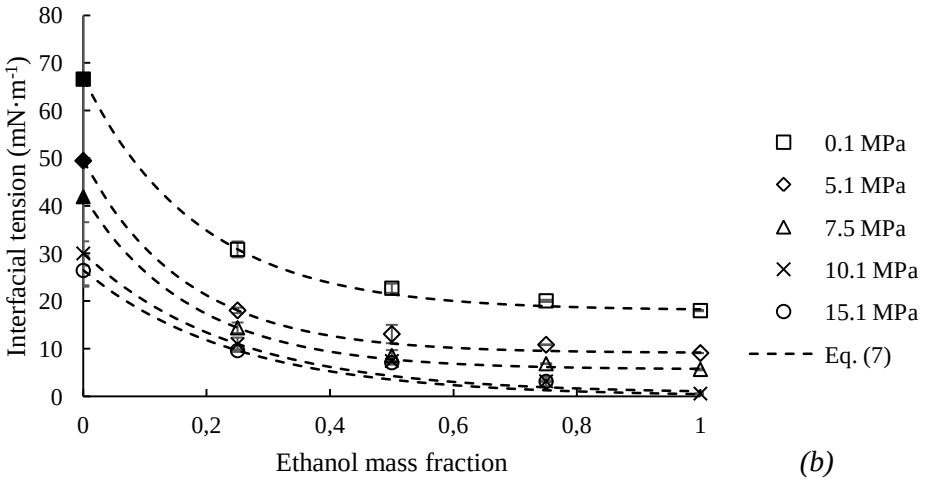

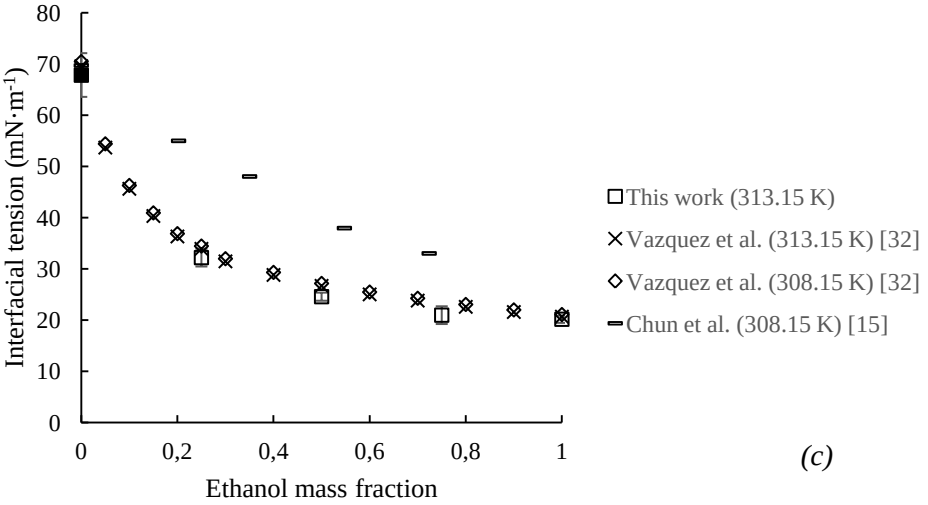

Fig. 7 Interfacial tension as function of ethanol mass fraction (a) at 313.15 K; (b) at 333.15 K; (c) at 0.1 MPa in air [32], and at 0.1 MPa in CO_2, this work and [15]; full symbol for CO_2/water interfacial tensions were extracted from literature [16,18,19,25]. Correlation is given by Eq. (7)

Such behavior has already been observed for several organic-aqueous mixtures under atmospheric conditions, including ethanol-water mixtures [32,49]. A preferential adsorption of the ethanol molecules on the surface layer has been suggested and measured [50,51]. Several predictive models taking this phenomenon into account have been developed and are briefly presented in the work of Tjahjono et al. [49]. It can be assumed that the same phenomenon operates under pressure, leading to the same tendency across all studied pressures. However, when increasing the pressure, the continuous phase, vapor or supercritical, could have more influence than under atmospheric conditions, especially because of transfer phenomena as discussed in the works of Sun et al. [29] and Sutjiadi-Sia et al. [12].

Interfacial tensions of ethanol-water mixtures have been measured by Vazquez et al. [32] under atmospheric conditions for several temperatures, while measurements under pressurized CO_2 were carried out by Chun et al. [15]. The literature data and those measured in this work at 0.1 MPa, and at 308.15 or 313.15 K are presented in Fig. 7(c). Our measurements at 0.1 MPa are in good agreement with data from Vazquez. Indeed, when comparing data at 0.1 MPa for ethanol and water, the interfacial tension is in the same range in air or CO_2, with lower values in CO_2 atmosphere. The same tendency is observed for ethanol-water mixtures under CO_2 atmosphere in this work. In contrast, data obtained by Chun et al. [15] are far greater and this difference is also observed under higher pressure. Discrepancies can be explained by different measuring and equilibration time methods in the work of Chun et al. [15]. In addition, densities used for interfacial tension calculation are not specified.

3.5 Data modeling

Several types of correlations, with adjustable parameters, have been proposed to describe interfacial tension behavior depending on pressure, for CO_2/water in the work of Georgiadis et al. [25], on density, for CO_2/ethanol in the work of Dittmar et al. [28], or ethanol composition for mixture interfacial tension at atmospheric condition in the work of Vazquez et al. [32].

For the very first-time, correlations involving the dispersive and the polar contributions of ethanol, and water surface tensions, respectively noted γ_L^d and γ_L^p, are proposed for the modeling of interfacial tension behavior through pressure, noted P, and carbon dioxide density, noted ρ_{CO2}. As shown in Table 1, the polar contribution of ethanol surface tension is minor, and CO_2/ethanol interfacial tension tends rapidly towards zero, while water polar contribution is major, and CO_2/water interfacial tension decreases first strongly then shows residual value according to pressure or density. These observations lead us to suppose that the dispersive contribution decreases significantly with pressure or density, while the polar one decreases less significantly with these parameters.

These assumptions lead to the Eq. (3) to describe CO_2/water and CO_2/ethanol interfacial tensions over the studied pressure range (Fig. 2 and Fig. 3), where α_p and λ_p are both adjustable parameters.

$$\boldsymbol{\gamma_{LF}(P) = \gamma_L^d . e^{-\lambda_p P^2} + \gamma_L^p . (1 - \alpha_p . \sqrt[3]{P})} \qquad (3)$$

Since no data have been found on surface tension polar and dispersive contributions of ethanol-water mixtures another similar correlation (Eq. (4)) was used to describe CO_2/ethanol-water mixtures interfacial tension over the studied pressure range (Fig. 4). Where γ_L^1 and γ_L^2 are two additional adjustable parameters, homogeneous to an interfacial tension. No relation can be thus established between the adjustable parameters and the polar and dispersive contributions without further measurements.

$$\boldsymbol{\gamma_{LF}(P) = \gamma_L^1 . e^{-\lambda_p P^2} + \ \gamma_L^2 . (1 - \alpha_p . \sqrt[3]{P})} \qquad (4)$$

Correlations in Eq. (3) and in Eq. (4) show good agreements with experimental data since average absolute deviations (AAD) are under 17%. Detailed parameters and AAD for both Eq. (3) and (4) are given in Supplementary files (C-Table 3 and C-Table 4, respectively).

Same assumptions lead to the Eq. (5) to describe interfacial tensions of ethanol and water in carbon dioxide over the studied density range (Fig. 6(a) and Fig. 6(b)), where α_ρ and λ_ρ are both adjustable parameters.

$$\boldsymbol{\gamma_{LF}(\rho_{CO_2}) = \gamma_L^d . e^{-\lambda_\rho . \rho_{CO_2}} + \ \gamma_L^p . (1 - \alpha_\rho . \sqrt[3]{\rho_{CO_2}})} \qquad (5)$$

Since dispersive and polar contributions of ethanol-water mixture surface tensions are not known, another correlation is proposed in Eq. (6) to describe interfacial tensions of these mixtures in CO_2 (Fig. 6(c)), where γ_L^I and γ_L^{II} are also fitted parameters on experimental data, as it has been done for γ_L^1 and γ_L^2.

$$\boldsymbol{\gamma_{LF}(\rho_{CO_2}) = \gamma_L^I . e^{-\lambda_\rho . \rho_{CO_2}} + \ \gamma_L^{II} . (1 - \alpha_\rho . \sqrt[3]{\rho_{CO_2}})} \qquad (6)$$

Both Eq. (5) and Eq. (6) accurately represent interfacial tension data since AAD are under 15%. Detailed parameters and AAD for both Eq. (5) and (6) are given in Supplementary files (C-Table 5 and C-Table 6, respectively).

These equations, Eq. (3), Eq. (4), Eq. (5) and Eq. (6), can be upgraded on the first hand by considering the temperature effect on surface tension contributions. Indeed, dispersive and polar contributions used for ethanol were taken at 293.15 K and for water at 311.15 K, because they are the closest values found in the literature. On the other hand, these correlations can also be upgraded thanks to the measurement of the polar and dispersive contributions of surface tensions for ethanol-water mixtures, that are measurable under atmospheric condition.

Starting from the observation of an exponential decrease in interfacial tension when ethanol mass fraction increases, another modeling work is proposed in (Eq. (7)) to describe interfacial tensions as a function of ethanol mass fraction (Fig. 7(a) and Fig. 7(b)), where $\gamma_{ethanol/CO_2}$ and γ_{water/CO_2} are respectively the interfacial tension of ethanol and water in carbon dioxide at the considered pressure and temperature, and λ_m is a dimensionless adjustable parameter.

$$\gamma_{LF}(\omega) = (\gamma_{water/CO_2} - \gamma_{ethanol/CO_2}).e^{-\lambda_m \omega} + \gamma_{ethanol/CO_2} \quad (7)$$

This type of correlation is in good agreement under pressures up to 7.5 MPa at 313.15 K and up to 10.1 MPa at 333.15 K, while under higher pressure, the few numbers of points coupled with low interfacial tension values lead to AAD higher than 20 %. Furthermore, Eq. (7) fits also the data obtained at atmospheric conditions by Vazquez et al. [32]. Detailed parameters and AAD for Eq. (7) are given in Supplementary files (C-Table 7).

In addition, an experimental design with response surface methodology was used to estimate interfacial tension overall the experimental domain of this work and is presented in the supplementary files D. This work was realized thanks to the Ellistat® software.

4. Conclusions

The three main advances of this work are: (i) experimental interfacial tension measurements of ethanol, water, and their mixtures in pressurized carbon dioxide; (ii) the introduction of the Widom line concept for a better understanding of interfacial phenomena; (iii) assumptions on the influence of the dispersive and polar contributions of the surface tension of a component on the interfacial tension behavior under pressurized CO_2, allowing new modeling.

Indeed, a full dataset of interfacial tensions of ethanol, water, and their mixtures under high pressure carbon dioxide at 313.15 K and 333.15 K was measured and is now available. If CO_2/ethanol and CO_2/water interfacial tensions have been well studied in previous works, there is only few papers about interfacial tension of ethanol-water mixtures under high pressure carbon dioxide. Measurements show good agreements with previous available literature for CO_2/ethanol [29–31] and CO_2/water systems [16,18,24,25,27,42]. In contrast, clear discrepancies are found for CO_2/ethanol-water mixtures regarding the only previous work [15]. Potential discrepancy sources for CO_2/water interfacial tensions were well discussed in the work of Bikkina et al. [27]. It can be highlighted that a specific experimental procedure has been used to ensure the saturation of the different phases.

For all systems, the interfacial tension decreases when the pressure increases following a two-step behavior for ethanol-water mixtures and water, as previously discussed in literature [12,24,25]. All the interpretations discussed in previous papers could be connected to the concept of the Widom line [47,48]. This latter is newly introduced in this work for the interpretation of interfacial tension behavior under high pressure CO_2. The temperature effect is discussed referring to literature data on water [25] and shows a complex influence on interfacial tension. Interfacial tensions of ethanol, water and their mixtures appear also dependent of the carbon dioxide density. Finally, interfacial tensions of ethanol-water mixtures decrease exponentially as the ethanol mass fraction increases from the value of CO_2/water interfacial tension to the one of CO_2/ethanol interfacial tension, in agreement with previous works under atmospheric conditions [32].

Furthermore, starting from the assumptions that the polar and dispersive contributions of the surface tension decrease differently according to pressure or density, several correlations have been developed. They allow a fair modeling of the interfacial tension of ethanol, water, and their mixtures through pressure or carbon dioxide density. Different modeling works have been previously proposed by Georgiadis et al. [25] for pressure dependence or by Dittmar et al. [30] for carbon dioxide density dependence. However, for the very first-time, correlations involving the polar and dispersive contributions of the surface tension are proposed. In addition, another modeling work is newly proposed to estimate the interfacial tension through ethanol mass fraction, for all conditions of this work. These correlations are easy to compute and implement for various supercritical carbon dioxide processes [6–10].

These new and reliable data on physicochemical properties for the CO_2-ethanol-water system can be useful for improving the knowledge of the role played by interfacial tension in supercritical carbon dioxide processes such as fractionation of water-ethanol mixtures and helpful for process design [7]. In addition, these measurements, coupled with contact angle measurements, are also essential to calculate the work of adhesion, thanks to the Young-Dupré equation, between a liquid and a solid which could be relevant for packed columns. Collecting these data is the purpose of a further study under investigation.

References

[1] T.K. Sherwood, G.H. Shipley, F.A.L. Holloway, Flooding Velocities in Packed Columns, Ind. Eng. Chem. 30 (1938) 765–769. https://doi.org/10.1021/ie50343a008.

[2] M. Raja Rao, C. Venkata Rao, Flooding rates in packed liquid extraction towers, Chemical Engineering Science. 9 (1958) 170–175. https://doi.org/10.1016/0009-2509(58)80009-3.

[3] C. Koncsag, A. Barbulescu, Liquid-Liquid Extraction with and without a Chemical Reaction, in: 2011. https://doi.org/10.5772/15229.

[4] Y. Sia, Interfacial Phenomena of Liquids in Contact with Dense CO2, (2005).

[5] A. Bejarano, P.C. Simões, J.M. del Valle, Fractionation technologies for liquid mixtures using dense carbon dioxide, The Journal of Supercritical Fluids. 107 (2016) 321–348. https://doi.org/10.1016/j.supflu.2015.09.021.

[6] N. Ganan, J. Morchain, S. Camy, J.-S. Condoret, Rate-based simulation of a high pressure counter-current packed column for supercritical CO 2 extraction of alcohol from dilute aqueous mixtures, Journal of Supercritical Fluids. 135 (2018) 168–179. https://doi.org/10.1016/j.supflu.2018.01.020.

[7] A. Pieck, C. Crampon, A. Fabien, E. Badens, A new correlation for predicting flooding point in supercritical fractionation packed columns, The Journal of Supercritical Fluids. 179 (2021) 105404. https://doi.org/10.1016/j.supflu.2021.105404.

[8] E. Carretier, E. Badens, P. Guichardon, O. Boutin, G. Charbit, Hydrodynamics of Supercritical Antisolvent Precipitation: Characterization and Influence on Particle Morphology, Ind. Eng. Chem. Res. 42 (2003) 331–338. https://doi.org/10.1021/ie020439v.

[9] E. Badens, O. Boutin, G. Charbit, Laminar jet dispersion and jet atomization in pressurized carbon dioxide, The Journal of Supercritical Fluids. 36 (2005) 81–90. https://doi.org/10.1016/j.supflu.2005.03.007.

[10] R. Guillaument, A. Erriguible, C. Aymonier, S. Marre, P. Subra-Paternault, Numerical simulation of dripping and jetting in supercritical fluids/liquid micro coflows, The Journal of Supercritical Fluids. 81 (2013) 15–22.

[11] T. Jaouhari, F. Zhang, T. Tassaing, S. Fery-Forgues, C. Aymonier, S. Marre, A. Erriguible, Process intensification for the synthesis of ultra-small organic nanoparticles with supercritical CO2 in a microfluidic system, Chemical Engineering Journal. 397 (2020) 125333. https://doi.org/10.1016/j.cej.2020.125333.

[12] Y. Sutjiadi-Sia, P. Jaeger, R. Eggers, Interfacial phenomena of aqueous systems in dense carbon dioxide, The Journal of Supercritical Fluids. 46 (2008) 272–279. https://doi.org/10.1016/j.supflu.2008.06.001.

[13] R. Massoudi, A.D. King, Effect of pressure on the surface tension of water. Adsorption of low molecular weight gases on water at 25.deg., J. Phys. Chem. 78 (1974) 2262–2266. https://doi.org/10.1021/j100615a017.

[14] C. Jho, D. Nealon, S. Shogbola, A.D. King, Effect of pressure on the surface tension of water: Adsorption of hydrocarbon gases and carbon dioxide on water at temperatures between 0 and 50°C, Journal of Colloid and Interface Science. 65 (1978) 141–154. https://doi.org/10.1016/0021-9797(78)90266-7.

[15] B.-S. Chun, G.T. Wilkinson, Interfacial tension in high-pressure carbon dioxide mixtures, Ind. Eng. Chem. Res. 34 (1995) 4371–4377. https://doi.org/10.1021/ie00039a029.

[16] A. Wesch, N. Dahmen, K. Ebert, J. Schön, Grenzflächenspannungen, Tropfengrößen und Kontaktwinkel im Zweiphasensystem H2O/CO2 bei Temperaturen von 298 bis 333 K und Drücken bis 30 MPa, Chemie Ingenieur Technik. 69 (1997) 942–946. https://doi.org/10.1002/cite.330690709.

[17] S.R.P. da Rocha, K.L. Harrison, K.P. Johnston, Effect of Surfactants on the Interfacial Tension and Emulsion Formation between Water and Carbon Dioxide, Langmuir. 15 (1999) 419–428. https://doi.org/10.1021/la980844k.

[18] A. Hebach, A. Oberhof, N. Dahmen, A. Kögel, H. Ederer, E. Dinjus, Interfacial Tension at Elevated PressuresMeasurements and Correlations in the Water + Carbon Dioxide System, J. Chem. Eng. Data. 47 (2002) 1540–1546. https://doi.org/10.1021/je025569p.

[19] F. Tewes, F. Boury, Thermodynamic and Dynamic Interfacial Properties of Binary Carbon Dioxide−Water Systems, J. Phys. Chem. B. 108 (2004) 2405–2412. https://doi.org/10.1021/jp030895c.

[20] J.-Y. Park, J.S. Lim, C.H. Yoon, C.H. Lee, K.P. Park, Effect of a Fluorinated Sodium Bis(2-ethylhexyl) Sulfosuccinate (Aerosol-OT, AOT) Analogue Surfactant on the Interfacial Tension of CO2 + Water and CO2 + Ni-Plating Solution in Near- and Supercritical CO2, J. Chem. Eng. Data. 50 (2005) 299–308. https://doi.org/10.1021/je0499667.

[21] P. Chiquet, J.-L. Daridon, D. Broseta, S. Thibeau, CO2/water interfacial tensions under pressure and temperature conditions of CO2 geological storage, Energy Conversion and Management. 48 (2006) 736–744. https://doi.org/10.1016/j.enconman.2006.09.011.

[22] T. Akutsu, Y. Yamaji, H. Yamaguchi, M. Watanabe, R. Jr, H. Inomata, Interfacial tension between water and high pressure CO2 in the presence of hydrocarbon surfactants, Fluid Phase Equilibria. 257 (2007) 163–168. https://doi.org/10.1016/j.fluid.2007.01.040.

[23] S. Bachu, D. Brant Bennion, Dependence of CO2 -brine interfacial tension on aquifer pressure, temperature and water salinity, Energy Procedia. 1 (2009) 3157–3164. https://doi.org/10.1016/j.egypro.2009.02.098.

[24] S. Bachu, D.B. Bennion, Interfacial Tension between CO2, Freshwater, and Brine in the Range of Pressure from (2 to 27) MPa, Temperature from (20 to 125) °C, and Water Salinity from (0 to 334 000) mg·L−1, J. Chem. Eng. Data. 54 (2009) 765–775. https://doi.org/10.1021/je800529x.

[25] A. Georgiadis, G. Maitland, J.P.M. Trusler, A. Bismarck, Interfacial Tension Measurements of the (H2O + CO2) System at Elevated Pressures and Temperatures, J. Chem. Eng. Data. 55 (2010) 4168–4175. https://doi.org/10.1021/je100198g.

[26] A. Georgiadis, F. Llovell, A. Bismarck, F.J. Blas, A. Galindo, G.C. Maitland, J.P.M. Trusler, G. Jackson, Interfacial tension measurements and modelling of (carbon dioxide+n-alkane) and (carbon dioxide+water) binary mixtures at elevated pressures and temperatures, The Journal of Supercritical Fluids. 55 (2010) 743–754. https://doi.org/10.1016/j.supflu.2010.09.028.

[27] P.K. Bikkina, O. Shoham, R. Uppaluri, Equilibrated Interfacial Tension Data of the CO2–Water System at High Pressures and Moderate Temperatures, J. Chem. Eng. Data. 56 (2011) 3725–3733. https://doi.org/10.1021/je200302h.

[28] D. Dittmar, S. Bijosono Oei, R. Eggers, Interfacial Tension and Density of Ethanol in Contact with Carbon Dioxide, Chemical Engineering & Technology. 25 (2002) 23–27. https://doi.org/10.1002/1521-4125(200201)25:1<23::AID-CEAT23>3.0.CO;2-8.

[29] Y. Sun, B.Y. Shekunov, Surface tension of ethanol in supercritical CO2, The Journal of Supercritical Fluids. 27 (2003) 73–83. https://doi.org/10.1016/S0896-8446(02)00184-5.

[30] D. Dittmar, A. Fredenhagen, S.B. Oei, R. Eggers, Interfacial tensions of ethanol–carbon dioxide and ethanol–nitrogen. Dependence of the interfacial tension on the fluid density—prerequisites and physical reasoning, Chemical Engineering Science. 58 (2003) 1223–1233. https://doi.org/10.1016/S0009-2509(02)00626-7.

[31] Z. Yang, M. Li, B. Peng, M. Lin, Z. Dong, Y. Ling, Interfacial Tension of CO2 and Organic Liquid under High Pressure and Temperature, Chinese Journal of Chemical Engineering. 22 (2014) 1302–1306. https://doi.org/10.1016/j.cjche.2014.09.042.

[32] G. Vazquez, E. Alvarez, J.M. Navaza, Surface Tension of Alcohol + Water from 20 to 50 °C, J. Chem. Eng. Data. 40 (1995) 611–614. https://doi.org/10.1021/je00019a016.

[33] M. Budich, G. Brunner, Supercritical fluid extraction of ethanol from aqueous solutions, The Journal of Supercritical Fluids. 25 (2003) 45–55. https://doi.org/10.1016/S0896-8446(02)00091-8.

[34] J.S. Lim, Y.-W. Lee, J.-D. Kim, Y.Y. Lee, H.-S. Chun, Mass-transfer and hydraulic characteristics in spray and packed extraction columns for supercritical carbon dioxide-ethanol-water system, The Journal of Supercritical Fluids. 8 (1995) 127–137. https://doi.org/10.1016/0896-8446(95)90025-X.

[35] C.A. Pieck, C. Crampon, F. Charton, E. Badens, Multi-scale experimental study and modeling of the supercritical fractionation process, The Journal of Supercritical Fluids. 105 (2015) 158–169. https://doi.org/10.1016/j.supflu.2015.01.021.

[36] J.N. Israelachvili, 17 - Adhesion and Wetting Phenomena, in: J.N. Israelachvili (Ed.), Intermolecular and Surface Forces (Third Edition), Third Edition, Academic Press, San Diego, 2011: pp. 415–467. https://doi.org/10.1016/B978-0-12-375182-9.10017-X.

[37] C.J. van Oss, Interfacial Forces in Aqueous Media, 2nd ed., CRC Press, Boca Raton, 2006. https://doi.org/10.1201/9781420015768.

[38] B. LE NEINDRE, Tensions superficielles et interfaciales, Techniques de l'ingénieur Constantes Mécaniques et Viscosité. base documentaire : TIB339DUO. (1993). https://www.techniques-ingenieur.fr/base-documentaire/sciences-fondamentales-th8/constantes-mecaniques-et-viscosite-42339210/tensions-superficielles-et-interfaciales-k475/.

[39] N. EUSTATHOPOULOS, E. RICCI, B. DREVET, Tension superficielle, Ref : TIP551WEB - "Étude et propriétés des métaux." (1999). https://www-techniques-ingenieur-fr.lama.univ-amu.fr/base-documentaire/tiamb-archives-etudes-et-proprietes-des-metaux/download/m67/2/tension-superficielle.html (accessed March 11, 2021).

[40] Teclis Scientific, 2020 Brochure Produit Teclis, (2020). www.teclis-scientific.com.

[41] P.-S. marquis de Laplace, Traité de Mécanique Céleste, Supplément au tome X, 1805. https://gallica.bnf.fr/ark:/12148/bpt6k77592z.

[42] P. Legout, G. Lefebvre, M. Bonnin, J.-C. Gimel, L. Benyahia, O. Colombani, B. Calvignac, Synthesis of PDMS-b-POEGMA Diblock Copolymers and Their Application for the

Thermoresponsive Stabilization of Water-Supercritical Carbon Dioxide Emulsions, Langmuir. 36 (2020) 12922–12932. https://doi.org/10.1021/acs.langmuir.0c02194.

[43] G. Watson, C.K. Zéberg-Mikkelsen, A. Baylaucq, C. Boned, High-Pressure Density Measurements for the Binary System Ethanol + Heptane, J. Chem. Eng. Data. 51 (2006) 112–118. https://doi.org/10.1021/je050261u.

[44] D. Pečar, V. Doleček, Volumetric properties of ethanol–water mixtures under high temperatures and pressures, Fluid Phase Equilibria. 230 (2005) 36–44. https://doi.org/10.1016/j.fluid.2004.11.019.

[45] Z.R. Hinton, N.J. Alvarez, Surface tensions at elevated pressure depend strongly on bulk phase saturation, J Colloid Interface Sci. 594 (2021) 681–689. https://doi.org/10.1016/j.jcis.2021.02.114.

[46] E. Santos, P.R. Waghmare, F. Temelli, Interfacial tension and equilibrium contact angle of corn oil on polished stainless steel in supercritical CO2 and N2, The Journal of Supercritical Fluids. 156 (2020) 104665. https://doi.org/10.1016/j.supflu.2019.104665.

[47] M.E. Fisher, B. Widom, Decay of Correlations in Linear Systems, The Journal of Chemical Physics. 50 (1969) 3756–3772. https://doi.org/10.1063/1.1671624.

[48] E.N. de Jesús, J. Torres-Arenas, A.L. Benavides, Widom line of real substances, Journal of Molecular Liquids. 322 (2021) 114529. https://doi.org/10.1016/j.molliq.2020.114529.

[49] M. Tjahjono, M. Garland, A new modified parachor model for predicting surface compositions of binary liquid mixtures. On the importance of surface volume representation, Journal of Colloid and Interface Science. 345 (2010) 528–537. https://doi.org/10.1016/j.jcis.2010.01.067.

[50] Z.X. Li, J.R. Lu, D.A. Styrkas, R.K. Thomas, A.R. Rennie, J. Penfold, The structure of the surface of ethanol/water mixtures, Molecular Physics. 80 (1993) 925–939. https://doi.org/10.1080/00268979300102771.

[51] G. Raina, G.U. Kulkarni, C. Rao, Surface Enrichment in Alcohol−Water Mixtures, (2001). https://doi.org/10.1021/JP011190I.

Figure captions

Table

Table 1 Surface tension of ethanol and water with dispersive and polar contributions

Liquid	Temperature (K)	γ_L ($mN \cdot m^{-1}$)	γ_L^d ($mN \cdot m^{-1}$)	γ_L^p ($mN \cdot m^{-1}$)
Ethanol	293.15	21.4	18.8	2.6
Water	293.15	72.8	21.8	51.0
	311.15	70.0	21.0	49.0

Supplementary Files

A. Complements to thermodynamical data

Densities used for interfacial tension calculation are given in Table 2 with statistical uncertainty. Please, refer to the 2.4 Measurement procedure for more details. Due to the rich literature about the interfacial tension of the CO_2/water system, only a few points were measured, and the water dataset was completed for further data calculations from literature. Interfacial tension measurements are summarized in Table 2 and the high uncertainty for water is due to the low number of measurements.

Table 2 Interfacial tension measurements of this work for water, ethanol, and their mixtures in CO_2 at various P and T

P (MPa)	T (K)	$\omega_{ethanol}$	γ_{LF} ($mN \cdot m^{-1}$)	ρ_{CO2} ($kg \cdot m^{-3}$)	ρ_{drop} ($kg \cdot m^{-3}$)
5.1	313.15	0	44.86 ± 2.02	116.3	994.4
10.1	313.15	0	32.85 ± 5.27	635.9	996.6
15.1	313.15	0	28.00 ± 3.63	781.8	998.7
0.1	313.15	0.25	32.15 ± 1.73	1.7	949.4
5.1	313.15	0.25	18.47 ± 1.27	116.3	951.4
7.5	313.15	0.25	11.89 ± 1.50	231.5	952.4
10.1	313.15	0.25	11.34 ± 0.25	635.9	953.5
15.1	313.15	0.25	9.34 ± 0.83	781.8	955.5
0.1	313.15	0.50	24.53 ± 0.79	1.7	897.5
5.1	313.15	0.50	12.44 ± 0.51	116.3	900.0
7.5	313.15	0.50	6.46 ± 1.55	231.5	901.2
10.1	313.15	0.50	6.69 ± 0.85	635.9	902.5

15.1	313.15	0.50	5.02	±	0.27	781.8	905.0
0.1	313.15	0.75	20.92	±	1.73	1.7	838.0
5.1	313.15	0.75	10.38	±	1.27	116.3	841.2
7.5	313.15	0.75	4.06	±	0.83	231.5	842.7
10.1	313.15	0.75	2.79	±	0.61	635.9	844.3
15.1	313.15	0.75	1.25	±	0.83	781.8	847.5
0.1	313.15	1	20.12	±	0.71	1.7	772.3
5.1	313.15	1	8.60	±	1.95	116.3	776.9
7.5	313.15	1	1.41	±	0.12	231.5	779.2
8.0	313.15	1	0.27	±	0.02	277.9	779.6
10.1	333.15	0	30.02	±	2.55	296.1	987.5
15.1	333.15	0	26.44	±	3.12	607.8	989.7
0.1	333.15	0.25	30.87	±	1.67	1.6	935.3
5.1	333.15	0.25	18.06	±	0.59	100.8	937.5
7.5	333.15	0.25	14.41	±	1.11	172.8	938.5
10.1	333.15	0.25	10.98	±	1.38	296.1	939.6
15.1	333.15	0.25	9.62	±	0.27	607.8	941.8
0.1	333.15	0.50	22.72	±	0.97	1.6	880.0
5.1	333.15	0.50	13.10	±	1.93	100.8	882.7
7.5	333.15	0.50	8.57	±	1.16	172.8	884.0
10.1	333.15	0.50	7.44	±	0.69	296.1	885.4
15.1	333.15	0.50	7.08	±	0.40	607.8	888.2
0.1	333.15	0.75	20.07	±	0.22	1.6	819.7
5.1	333.15	0.75	10.85	±	0.08	100.8	823.1
7.5	333.15	0.75	6.88	±	0.04	172.8	824.8
10.1	333.15	0.75	3.17	±	0.19	296.1	826.6
15.1	333.15	0.75	3.14	±	0.98	607.8	830.1
0.1	333.15	1	18.01	±	0.11	1.6	754.2
5.1	333.15	1	9.10	±	0.03	100.8	759.4
7.5	333.15	1	5.67	±	0.19	172.8	762.0
10.1	333.15	1	0.59	±	0.03	296.13	764.6

B. Literature data discussion

It is important to note that five sources of discrepancies have been pointed out in the literature and might explain the differences between the literature data. (I) Discrepancies could originate from density values used to calculate the interfacial tension. Although pure component densities at given pressure and temperature are often used, transfer between the drop and continuous phases under high pressure can significantly change the density values, as discussed for CO_2/water system in the work of Bikkina et al. [27]. (II) As shown in the work of Hebach et al. [18], the temperature measurement location in the apparatus and the precision might affect the estimation of interfacial tension, mainly in conditions near the critical point of carbon dioxide. Other discrepancy sources could be (III) different balancing times and "equilibrium state" [45], (IV) different methods/apparatus, or else (V) the presence of impurities (seal dissolution etc.) that can lower the interfacial tension [27].

Measurements are in good agreement with the literature for the CO_2/ethanol system, except with Sun et al. [29] at 333.15 K whose values are lower than those given in Dittmar et al. and Yang et al. [30,31] and those measured in this work. Dittmar et al. [30] used pure density, like this work, Yang et al. [31] measured pure density at working temperature, considering the fluid as incompressible, while Sun et al. [29] used the calculated density of saturated ethanol, that could explain the difference.

Regarding the CO_2/water system, discrepancies are greater at 313,15 K than at 333.15 K, which agrees with discrepancy sources (I-II) cited above. Most of the literature data presented are estimated using pure density, except Bachu et al. and Bikkina et al. [24,27] who used respectively measured and calculated density of saturated water. Longer balancing times was applied in the work of Tewes et al. and Bikkina et al. [19,27]. Concerning the "equilibrium state", reaching the true thermodynamical equilibrium remains current questioning in the interface science community. Recent work [45], showing new experimental set-up that allow quick equilibrium, has presented results in agreement with Tewes et al. [19] for pressure up to 5.72 MPa at 295.65 K.

C. Complements to modeling data

Concerning Eq.(3):

- for CO_2/ethanol, data from this work were only used for fitting and AAD calculation,

- for CO_2/water at 313.15 K, only data from the literature were used except those from the work of Tewes et al. [16,24,25,27]; indeed, it follows the same tendency (two-step behavior) but with much lower values than the rest of the literature as discussed in the complementary file B,

- for CO_2/water at 333.15 K, the complete set of data from the literature was used [16,18,24,25,27]. Details are given in Table 3.

Table 3 Detailed parameters and AAD for Eq. (3) applied to CO_2/ethanol and CO_2/water systems

System	Temperature (K)	γ_L^d ($mN \cdot m^{-1}$)	γ_L^p ($mN \cdot m^{-1}$)	λ_p (MPa^{-2})	α_p ($MPa^{-1/3}$)	AAD (%)
CO_2/Ethanol	*313.15*	*18.8*	*2.6*	0.0197	1.4503	13%
	333.15	*18.8*	*2.6*	0.0057	2.1718	17%
CO_2/Water	*313.15*	*21.0*	*49.0*	0.0230	0.2019	9.7%
	333.15	*21.0*	*49.0*	0.0181	0.1641	4.3%

Concerning Eq.(4), details are given in Table 4

Table 4 Detailed parameters and AAD for Eq. (4) applied to CO_2/ethanol-water mixtures

$\omega_{ethanol}$	Temperature (K)	γ_L^1 ($mN \cdot m^{-1}$)	γ_L^2 ($mN \cdot m^{-1}$)	λ_p (MPa^{-2})	α_p ($MPa^{-1/3}$)	AAD (%)
ω = 0.25	*313.15*	16.9	17.6	0.0342	0.1904	3%
	333.15	15.1	17.2	0.0345	0.1782	2%

ω = 0.50	*313.15*	15.0	10.6	0.0371	0.2117	7%
	333.15	15.1	7.7	0.0393	0.0321	1%
ω = 0.75	*313.15*	17.9	3.5	0.0287	0.2613	8%
	333.15	15.3	5.1	0.0295	0.1574	7%

Concerning Eq.(5), details are given in Table 5

Table 5 Detailed parameters and AAD for Eq. (5) applied to CO_2/ethanol and CO_2/water systems

System	γ_L^d $(mN \cdot m^{-1})$	γ_L^p $(mN \cdot m^{-1})$	λ_ρ $(m^3 \cdot kg^{-1})$	α_ρ $(kg \cdot m^3)^{-1/3}$	***AAD*** ***(%)***
CO_2/ethanol	18.8	2.6	0.0052	0.3682	9.9%
CO_2/water	21.0	49.0	0.0090	0.0513	5%

Concerning Eq.(6), details are given in Table 6

Table 6 Detailed parameters and AAD for Eq. (6) applied to CO_2/ethanol-water mixtures

$\omega_{ethanol}$	γ_L^I $(mN \cdot m^{-1})$	γ_L^{II} $(mN \cdot m^{-1})$	λ_ρ (MPa^{-2})	α_ρ $(MPa^{-1/3})$	***AAD*** ***(%)***
ω = 0.25	21.3	11.2	0.0100	0.0178	3%
ω = 0.50	19.8	5.0	0.0088	0	10%
ω = 0.75	18.3	3.1	0.0076	0.0667	15%

Concerning Eq.(7), details are given in Table 7

*Table 7 Detailed parameters and AAD for Eq. (7) ; [a] average value from[16,19], [b] average value from[16,18], [c] values from or interpolated from [25], * values assumed to be null*

Temperature (K)	**Pressure (MPa)**	$\gamma_{water/CO2}$ $(mN \cdot m^{-1})$	$\gamma_{ethanol/CO2}$ $(mN \cdot m^{-1})$	λ_m	**AAD (%)**
313.15	0.1	67.80[a]	20.12	5.508	1.3%
	5.1	44.86	8.19	5.088	5.4%
	7.5	35.17[c]	1.41	4.679	18.1%

	10.1	32.85	0*	4.254	23.3%
	15.1	28.00	0*	4.390	13.7%
	0.1	66.60[b]	18.01	5.319	2.6%
	5.1	49.49[c]	9.10	6.023	5.7%
333.15	7.5	41.92[c]	5.67	5.690	4.3%
	10.1	30.02	0.59	4.166	32.1%
	15.1	26.44	0*	4.044	27.5%

D. Experimental design

Concerning experimental design, in the present work, interfacial tension measurements were performed under pressures of 0.1, 5.1, 10.1 and 15.1 MPa, and at temperatures of 313.15 and 333.15 K, which cover the frequent operating range adopted for ethanol-water SC-CO_2 fractionation, for five ethanol-water mixtures with an ethanol mass fraction ω of 0, 0.25, 0.50, 0.75 and 1. Additional measurements were realized near the critical point of CO_2 at 7.5 MPa.

To study the influence of parameters Pressure (P), Temperature (T), and ethanol mass fraction (ω), and in order to describe interfacial tension in the range of studied conditions, an experimental design with response surface methodology was implemented using Ellistat software. The three factors P, T, ω, were chosen as entry values with five pressure levels, two temperature levels and five composition levels. An example of response surface generated with this software is shown in Fig. 8.

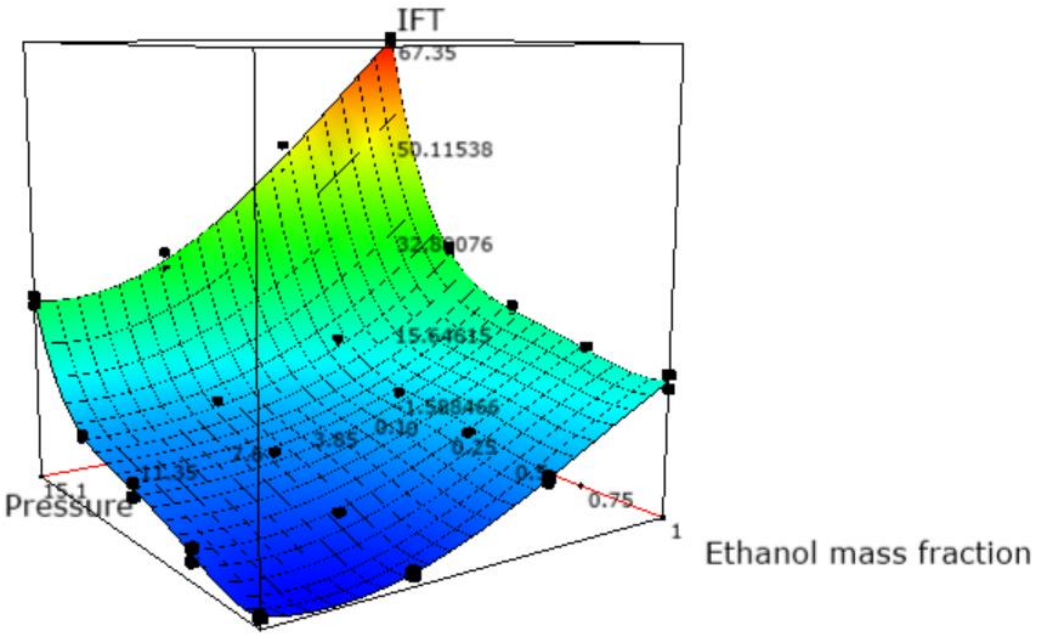

Fig. 8 Response surface at 323.15 K generated with Ellistat

The response surface is generated with a matrix model with R^2=99.5%. This tool enables the targeting of a specific value of the response thanks to a complete dataset on the operatory conditions.